

Kushe Tincture Ameliorates DNCB-Induced Atopic Dermatitis by Affecting NF-Kb/JAK-STAT3 Pathway: Bioinformatics Analysis and Animal Experiment Verification

Huishang Feng^{1,2}, Yang Zhou³, Xuwen Ren⁴, Xintian Zhu⁵, Xingwu Duan¹, Shuangqing Qu¹, Baochen Zhu⁶, Yuanwen Li^{2,7}, Yeping Qin⁸

¹Department of Dermatology, Dongzhimen Hospital Beijing University of Chinese Medicine, Beijing, People's Republic of China; ²Second Clinical Medical School, Beijing University of Chinese Medicine, Beijing, People's Republic of China; ³Beijing University of Chinese Medicine, Beijing, People's Republic of China; ⁴Shanxi Traditional Chinese Medical Hospital, Taiyuan, Shanxi, People's Republic of China; ⁵School of Chinese Materia Medica, Beijing University of Chinese Medicine, Beijing, People's Republic of China; ⁶Department of Pharmacy, Dongzhimen Hospital Beijing University of Chinese Medicine, Beijing, People's Republic of China; ⁷Department of Dermatology, Dongfang Hospital, Beijing University of Chinese Medicine, Beijing, People's Republic of China; ⁸Department of Dermatology, Chongqing Traditional Chinese Medicine Hospital, Chongqing, People's Republic of China

Correspondence: Yuanwen Li, Department of Dermatology, Dongfang Hospital, Beijing University of Chinese Medicine, No. 6 Fangxingyuan Fengtai District, Beijing, 100078, People's Republic of China, Email 15810104902@163.com; Yeping Qin, Department of Dermatology, Chongqing Traditional Chinese Medicine Hospital, No. 40, Daomenkou, Yuzhong District, Chongqing, 400011, People's Republic of China, Email qinyeping92@163.com

Background: Kushe tincture (KSD), an optimized in-hospital preparation of Dongzhimen Hospital of Beijing University of Traditional Chinese Medicine, has been clinically used as an anti-inflammatory and anti-itching topical therapeutic drug for the treatment of eczema, atopic dermatitis (AD) and so on for decades. However, the potential therapeutic mechanisms remained unexplored.

Objective: This study aimed to explore the mechanisms underlying the therapeutic effects of KSD against DNCB-induced AD through the combination of single-cell RNA sequencing (scRNA-seq), spatial transcriptomics (ST), and animal experiments.

Methods: Firstly, we collected the active components and targets of KSD from the Traditional Chinese Medicine Systems Pharmacology (TCMSP) and obtained AD-associated targets from the Gene Expression Omnibus (GEO) database. Protein-protein interaction (PPI) networks were constructed using Cytoscape with Kyoto Encyclopedia of Genes and Genomes (KEGG) analyses. Secondly, core targets were screened and visualized by scRNA-seq and ST technology. Finally, we adopted DNCB-induced AD-like mouse model to observe the therapeutic effect of KSD through lesion scoring, morphological staining, serological tests, skin barrier function measurements, flow cytometry, and Western blotting.

Results: Forty-six common drug-disease targets were obtained and top 2 ranked targets were chosen, namely NF-kB1 and STAT3. Combined scRNA-seq and ST suggested that NF-KB and STAT3 had higher and wider expression in most subpopulations, especially in monocytes and CD4⁺ T-cells. Animal experiments showed that KSD treatment improved the visible symptoms and skin barrier function and decreased mast cell infiltration, IgE levels, Th17 cells, and expression of NF-kB, JAK2, and STAT3.

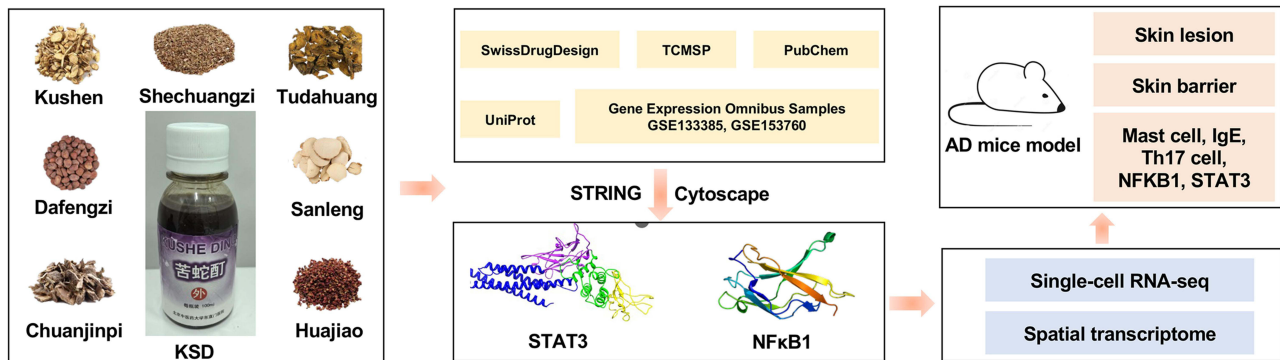
Conclusion: KSD has therapeutic effects on DNCB-induced AD-like skin lesions, and it has effects on NF-kB and JAK-STAT3 proteins, which may be possible targets.

Keywords: single-cell RNA sequencing, spatial transcriptomics, kushe tincture, NF-kB signaling pathway, JAK-STAT3 signaling pathway, AD mouse model

Introduction

Atopic dermatitis (AD), also referred to as eczema, atopic eczema, and hereditary allergic dermatitis, is a recurrent pruritic inflammatory skin disease with a genetic predisposition,¹ affecting 20% of children and 3% of adults worldwide.² AD is prevalent in infants and children and can continue into adulthood or adult seizures, which are typically characterized by acute skin inflammation of the face and extensor sides in infancy and childhood, followed by chronic inflammation of the flexor sides and

Graphical Abstract



features such as mossification and scaling in adulthood. It was reported that the prevalence of AD in China reached 30.48% in infancy, 12.94% in preschool children, and 0.6% in adults.³ Although AD is not fatal, it often leads to complications, such as itching, lack of sleep, social embarrassment, and depression due to noticeable skin lesions, which can significantly impact patients' physical and mental well-being.⁴ Therefore, there is an urgent need to develop additional therapeutic agents.

Traditional Chinese Medicine (TCM) has a long history of improving health in China and is likely to represent inspiration for the treatment of AD. Kushe Tincture (KSD), an optimized in-hospital preparation of Dongzhimen Hospital of Beijing University of Traditional Chinese Medicine, was developed in the 1980s by the famous dermatologist Jin Qifeng.⁵ For decades, its efficacy has received considerable attention in a large number of patients. In TCM, the combination of the aforementioned herbs could function on clearing heat, drying dampness, detoxifying, relieving itching and killing insects. Therefore, it was and has been commonly used as an anti-inflammatory and anti-itching topical therapeutic drug for the treatment of eczema, psoriasis, pruritus, seborrheic dermatitis and so on.⁶ Recently, studies have confirmed the anti-inflammatory effects of herbs used in KSD. The primary component of *Sophora flavescens* Aiton (Kushen), OMT, has numerous pharmacological effects, including antioxidant,⁷ antifibrotic,⁸ and anti-inflammatory properties.⁹ *Cnidium monnieri* (L.) Cuss. (Shechuangzi) has been reported to exert anti-inflammatory, anti-allergic activities.¹⁰ Notably, corynoline is a component of *Zanthoxylum bungeanum* Maxim. (Huajiao), inhibited the NF-κB pathway.¹¹ These effects may be contributed to the anti-inflammatory properties of KSD, a multi-herb external preparation. To this day, it remains a "treasure" in the hearts of both doctors and patients. In addition, because of the intricate nature of Chinese materia medicas, the exact mechanism by which it treats AD remains unclear.

Bioinformatics analysis, particularly network pharmacology, single-cell RNA sequencing (scRNA-seq), and spatial transcriptomics (ST), is providing new perspectives and tools for target prediction and treatment strategy development in the treatment of AD with TCM. For example, through scRNA-seq of AD skin lesions, researchers discovered specific clusters of fibroblasts, dendritic cells, and macrophages, which play a key role in the infiltration and interaction of lesions.¹² Network pharmacology combined with transcriptomic analysis suggests that EMW alleviates AD symptoms by inhibiting the MAPK signaling pathway and activating the EGFR/AKT signaling pathway.¹³ Additionally, research combining scRNA-seq with computational frameworks has also provided new perspectives for the diagnosis and treatment of AD.¹⁴ Through these technologies, we can gain a deeper understanding of the complex pathological mechanisms of AD, and provide theoretical support for the clinical application of TCM.

In our study, we explored the potential mechanism of KSD in the treatment of AD. Through scRNA-seq and ST technology, TNF-NF-κB and JAK-STAT signaling pathways were focused. Subsequent animal experiments employing DNCB-induced mice models were conducted to validate, explaining the molecular mechanism of KSD. We hope to open a new way of thinking for the treatment of pure Chinese herbal medicine for AD and lay the foundation for the subsequent clinical application of this product.

Materials and Methods

Bioinformatics Analysis

Screening of Active Ingredients in KSD and Target Prediction

Based on the Chinese Pharmacopoeia and Traditional Chinese Medicine System Pharmacology Analysis Platform (TCMSP, <http://lsp.nwu.edu.cn/tcmsp.php>), active ingredients in KSD (*Zanthoxylum bungeanum* Maxim. (Huajiao), *Hibiscus syriacus* L. (Chuanjinpi), *Rumex obtusifolius* L. (Tudahuang), *Hydnocarpus anthelmintica* Pierre (Dafengzi), *Sparganium stoloniferum* Buch.-Ham. (Sanleng), *Sophora flavescens* Ait. (Kushen), *Cnidium monnieri* (L.) Cuss. (Shechuangzi)) were screened using drug likeness ($DL \geq 0.18$) and lipid-water partition coefficient < 0.3 . To avoid excluding certain well-recognized active components, we simultaneously referenced the Chinese Pharmacopoeia (2015 edition) and relevant literature to identify such components. The corresponding protein targets were obtained by TCMSP database and PubChem database (<https://pubchem.ncbi.nlm.nih.gov>), and the names of the targets were standardized using the UNIPROT database (<https://www.uniprot.org>) with species restriction as human. Swiss Target Prediction (<http://www.swisstarget-prediction.ch/>) was used to predict the targets of KSD targets.

Acquisition of Genes Associated with AD

The dataset used in this study was obtained from the Gene Expression Omnibus (GEO) database. The selection criteria included the inclusion of samples from patients with AD and healthy controls, a sufficient sample size, and data types covering whole-transcriptome expression information. The GSE133385 and GSE153760 datasets were selected for subsequent analyses. The downloaded raw data were subjected to background correction, standardization, and data filtering. Microarray data were analyzed for differential expression using the limma package in the R software to compare gene expression differences between the AD and healthy control groups. The screening threshold was set at an adjusted P-value < 0.05 and $|\log_2 \text{Fold Change}| > 1$ to identify disease-associated genes for atopic dermatitis.

Target Identification and Network Construction for AD

Drug targets obtained from the TCMSP database and disease targets obtained from the GEO database were imported into Venny 2.0, to generate common target genes. The STRING online database (<https://string-db.org/>) was used to obtain protein-protein interaction (PPI) networks and KEGG pathway maps. The obtained protein interaction data were imported into the Cytoscape software to obtain core targets with the highest degree values.

Single-Cell Sequencing Analysis

The dataset GSE153760 was downloaded from the GEO database and single-cell transcriptome data were analyzed using R software (version 1.4.2) in conjunction with the “Seurat” package. First, the merge function in the “Seurat” package was used to merge data from multiple samples and perform preliminary screening to exclude genes with low expression levels and retain cells with $n\text{Feature_RNA} > 40$ and $n\text{Count_RNA} > 3$. Next, samples meeting the following conditions: $n\text{Feature_RNA} > 300$, $n\text{Count_RNA} > 1000$ and $\text{percent.mt} < 20$ were screened to ensure the data quality met the analysis requirements. Subsequently, all gene expression data were normalized and scaled using the ScaleData function to ensure that each gene had zero mean and unit variances. To further explore the heterogeneity of the cell populations, principal component analysis (PCA) and uniform manifold approximation and projection (UMAP) were performed, and the top 20 principal components were selected for subsequent analyses, setting $\text{reduction} = 1$ to visualize the distribution of different cell populations. Cell type annotation was done by “SingleR” package, and DEGs across cell clusters were identified using the FindAllMarkers function. Cell identities were determined by examining the canonical marker genes. In addition, based on the MSigDB (Molecular Signatures Database), we downloaded the “KEGG_MEDICUS_REFERENCE_CYTOKINE_JAK_STAT_SIGNALING_PATHWAY” and “KEGG_MEDICUS_REFERENCE_TNF_NFKB_SIGNALING_PATHWAY” gene sets, which were scored using the AUCcell method and visualized to investigate their expression characteristics in the cell population.

Spatial Transcriptome Data Processing and Analysis

The GSE197023 microarray files were downloaded from the GEO database, and the raw gene expression matrix was extracted and the spatial coordinate information was integrated (Read10X_Image) using Read10X in the R software (version 1.4.2). After constructing an independent Seurat object for each sample, the SCTransform algorithm was used to

normalize the data to eliminate technical variability and create a unified analysis dataset. Cell clustering was accomplished using PCA dimensionality reduction analysis combined with UMAP nonlinear visualization using the shared nearest neighbor (SNN) modular optimization algorithm. Inter-cluster differential genes were screened using FindAllMarkers (threshold: $|\log_2FC| > 1$, corrected p-value < 0.05), and the pseudo-volume method was used to quantify inter-group expression differences between AD and control groups. The spatial distribution patterns of the key genes were visualized using SpatialFeaturePlot.

Animal Experiment

Reagents

KSD and KSD alcoholic extract (aeKSD) (Z20053160) were prepared by the Preparation Room of Dongzhimen Hospital, Beijing University of Traditional Chinese Medicine, according to the standard for the execution of in-hospital preparations. It was composed of seven herbs, namely *Zanthoxylum bungeanum* Maxim. (Huaajiao), *Hibiscus syriacus* L. (Chuanjinpi), *Rumex obtusifolius* L. (Tudahuang), *Hydnocarpus anthelmintica* Pierre (Dafengzi), *Sparganium stoloniferum* Buch-Ham. (Sanleng), *Sophora flavescens* Ait. (Kushen) and *Cnidium monnieri* (L.) Cuss. (Shechuangzi) software. The dosage of this preparation has not been disclosed to the public because of the subsequent patent applications. Plant names were checked using MPNS (<http://mpns.kew.org>).

1-chloro-2,4-dinitrobenzene (DNCB, 138630) and acetone (179124) were purchased from Sigma-Aldrich (St Louis, MO, USA). Hydrocortisone Butyrate Cream (HB, H10940095) was obtained from Tianjin Jin Yao Pharmaceutical Co., Ltd (Tianjin, China). Mouse helper Th1/Th2 cell assay kits (KTH201, KTH217) were purchased from Lianke Bio (Hangzhou, China). RPMI1640 complete medium (11875), high-efficiency RIPA lysate (R0010), phenylmethanesulfonyl fluoride (PMSF) (R0100), loading buffer (P1040), BCA protein assay kit (PC0020) was purchased from Solaibao (Beijing, China). Fetal bovine serum (FBS) was purchased from Gibco (New York, USA). Mouse IgE ELISA Assay Kit (CME0029) was obtained from 4A Biotech (Suzhou, China). Anti-phospho-NF- κ B (82335-1-RR), anti-NF- κ B (10745-1-AP), anti-phospho-STAT3 (28,945-1-AP), anti-STAT3 (10,253-2-AP) and anti- β -actin (66009-1-Ig) were purchased from Proteintech (Wuhan, China). Anti-phospho-JAK2 (3771) and anti-JAK2 (3230) were purchased from Cell Signaling Technology (Danvers, USA).

Animal Modeling and Interventions

Thirty 6-week-old SPF-grade female BALB/c mice (22 ± 2 g) were purchased from Beijing SiPeiFu Bio-Technology Co., Ltd (SCXK (Beijing) 2019-0010), and all the mice were housed in an environment with temperature: (22 ± 1) °C, ambient humidity 55–65%, and a 12-h light/dark cycle, with free access to drinking water and food every day. The animal study was reviewed and approved by the ethics committee of Beijing MDKN Biotechnology Co., Ltd (Approval No. MDKN-2022-079).

DNCB was used to construct AD model based on previous publication with minor modification.¹⁵ The hair on the dorsal skin was shaved and the skin recovered for 24 h. Briefly, DNCB was solubilized in acetone/olive oil/alcohol (2/1/1, v/v/v) to prepare 0.5% (w/v) and 1.0% (w/v) DNCB solution, respectively. The mouse was sensitized by 200 μ L of 0.5% (w/v) DNCB onto the shaved dorsal skin. The sensitization was performed on days 1, 4, 7. After the sensitization, 200 μ L of 1.0% (w/v) DNCB were repeatedly applied to the sensitized dorsal skin, on days 10, 13, 16, 19, 22, 25 and 28 for challenge.

Considering that the KSD is an in-hospital preparations for external use, only a single dose was set in animal experiments that was the same as clinical dose. Based on power analysis conducted from preliminary studies, mice were randomly divided into 5 groups using random number table (6 mice per group) as follows: 1) control: healthy mice with no treatment; 2) Mode: DNCB-induced mice without drug treatment; 3) KSD: DNCB-induced mice with topical application of KSD daily (0.15 g/mL, 0.4 mL); 4) aeKSD: DNCB-induced mice with topical application of aeKSD daily (0.15 g/mL, 0.4 mL); 5) HB: DNCB-induced mice with topical application of HB daily (0.4 g). To reduce possible confounding factors, all animals were treated at the same time each day, and order of treatments, measurements and caging of animal was random. At the end of the experiments, mice were weighted. Mice were anesthetized by intraperitoneal administration of 0.3% pentobarbital sodium (0.1mL/10g), blood samples were taken from the abdominal aorta and sacrificed by cervical dislocation. Direct cardiac palpation was performed to confirm the death of mice. After

mice were sacrificed, the treated dorsal skin was subjected to histopathological and immunohistochemical analyses. Spleen was weighted to calculate the spleen index (spleen weight/body weight). Blood samples were collected and centrifuged at 1600 g for 15 min at 4°C to obtain serum.

Skin Lesion Scoring

Skin lesions on the backs of mice were scored on days 0, 7, 14, and 28 of the experiment, with reference to the Scoring atopic dermatitis (SCORAD) criteria proposed by the European AD group.¹⁶ The severity of the skin on the back of the mice was scored by three experimenters at a time to obtain the average value in order to exclude subjective effects.

Hematoxylin-Eosin (HE) Staining of Skin, Liver and Kidney

HE staining was performed according to standard histological protocols. After dewaxing, slices were incubated with hematoxylin for 2 min and thereafter stained with eosin. Subsequently, alcohol was used to dehydrate the sections, which were then made transparent with xylene and sealed with gum solution.

Toluidine-Blue Staining

Mouse dorsal skin tissues from each group were sectioned, deparaffinized, stained with Toluidine-blue, rinsed with distilled water, ethanol-differentiated, dehydrated and transparent and then sealed. The infiltration of mast cells in each tissue was observed using an electron microscope and images were captured for analysis and statistics.

Spleen Index

After the mice were killed by cervical dislocation 24 h after the last day of the experiment, the mice were weighed and their spleens were removed, and their mass was weighed to calculate the spleen index (spleen index = spleen mass/body mass).

ELISA for Serum IgE Detection

Blood was taken from the heart of mice, serum was prepared, and the kit instructions were followed in order to detect the level of IgE in serum. A standard curve was performed using Curve expert 1.4 and the concentration of each sample was calculated from the optical density (OD) value of the sample.

Flow Cytometric Detection of Spleen Th17 Cell Levels

Spleens were harvested and single-cell suspensions were prepared by gentle grinding between sterile ground glass slides. After centrifugation and resuspension in RPMI1640 complete medium, cells were stimulated with phorbol myristate acetate/ionomycin/GolgiStop for 4 h. Add CD3 PercP/CD4 FITC according to the recommended amount of antibody and incubate for 15 min with mixing and avoiding light. Add 1 mL fixed membrane-breaking agent and incubate for 15 min with mixing and avoiding light. At the end of the process, terminate the membrane-breaking by adding 1 mL buffer and centrifuging for 5 min at 1500rpm, and then discard the supernatant. Then, add IL-17A according to the recommended amount of antibody, mix well and incubate for 30 min, add 2 mL buffer, centrifuge at 1500rpm for 5 min, discard the supernatant. Add 300 ul buffer and run the test. The results were analyzed by CellQUEST Pro software.

Western Blot (WB) Assay

Protein was extracted from skin tissues by adding protease inhibitors with RIPA lysate. Samples containing 30 µg of protein were separated on 7.5% gel and transferred to a PVDF membrane, followed by 5% milk and incubation with antibodies against phospho-NF-κB (1:2500), NF-κB (1:1000), phospho-JAK2 (1:1000), JAK2 (1:1000), phospho-STAT3 (1:1000), STAT3 (1:1000) and β-actin (1:2000) overnight at 4°C. After three TBST washes, the PVDF membrane was incubated with the secondary antibody (1:10000) for 1 h at room temperature. Luminescence detection was performed with the ECL system and analyzed by Image J software.

Liver and Kidney Indicators

Mouse blood samples were centrifuged at room temperature, 3000 rpm for 15 min and the upper serum layer was removed. Alanine aminotransferase (ALT), aspartate transaminase (AST), blood urine nitrogen (BUN) and creatinine (CER) in mice serum were measured using Beckman Automated Biochemical Analyser AU5800.

Statistical Methods and Processing

For the part of scRNA-seq and spatial transcriptome, data analyses for this experiment were performed using multiple linear regression models to explore the association between independent variables and outcome variables. Subvariate splitting was performed by dummy variable coding for categorical variables, and biologically representative categories were used as reference groups. Data were analyzed using Stata 17.0 software (StataCorp LP) and regression results are presented as beta coefficients and their 95% confidence intervals.

For the part of animal experiment, Graphpad Prism 7.0 software was used for data analyses. To compare among groups, a one-way analysis of variance was employed, while the *t* test was utilized for comparisons between groups. Data were presented as mean \pm SD with $p < 0.05$ or $p < 0.01$ indicating statistical significance. To reduce subjective judgement, different people in team was responsible for allocation, experimental implementation, outcome assessment and data analysis, respectively.

Results

Active Ingredients in KSD and Potential Targets Prediction

In the TCMSP database, a total of 260 active ingredients were obtained in KSD after screening according to the criteria ($DL \geq 0.18$, lipid-water partition coefficient < 0.3) and removing duplicates. Two hundred and twenty-six targets of these active ingredients were collected from TCMSP database. A total of 2655 differential genes were obtained, of which 1346 were up-regulated and 1309 were down-regulated. Forty-six common drug-disease targets were obtained by intersecting the 266 drug targets with 2655 disease targets through Venny online platform.

Construction and Analysis of Core Targets

PPI network diagram was obtained after importing the aforementioned 46 shared targets into STRING database. The PPI data was exported in a basic text format (.tsv), and the TSV file was then imported into Cytoscape 3.9.0 to generate the target interaction network diagram. The top 2 most important targets were NF- κ B1 and STAT3 according to Degree value (Figure 1A). Then, the top 2 targets were analyzed for KEGG enrichment. Based on the number of genes enriched in each function, bar graphs (where the higher the number of enriched genes, the longer the bar graphs) were plotted by an online tool (Figure 1B). It was revealed that NF- κ B1, STAT3 and related signaling pathways might be vital targets for KSD in the treatment of AD.

ScRNA-Seq Analysis and ST Analysis

Single cell sequencing data (GSE153760) generated from the patient AD model was analyzed by a standardized process and 11 subpopulations were identified by t-SNE downscaling, including keratinocytes, monocytes, CD4⁺ T cells, dendritic cells (DC), melanocytes, endothelial cells, fibroblasts, natural killer cells (NK), hematopoietic stem cells (HSC), CD8⁺ T cells, and T cells. The cell distribution was detailed in Figure 1C.

Next, the previously screened STAT and NFKB1 as target genes were matched with each cellular subpopulation in the skin, and the distribution of gene expression was depicted in t-SNE downscaled plots. It can be seen that STAT and NFKB1 were widely expressed in most of the subpopulations and had higher levels in the AD group. Among them, NFKB1 was mainly expressed in the monocyte subpopulation, while STAT3 was mainly expressed in the monocyte subpopulation and the CD4⁺ T cell subpopulation (Figure 1D).

Based on the differential gene suggestion in the microarray data from the GEO database (GSE197023), the expression levels of NF κ B and STAT3 in the epidermal tissues of patients with atopic dermatitis (AD) showed a tendency to be up-regulated compared with those of the healthy control group. Specifically, the whole epidermal layer of pathological sections in the healthy group showed mostly blue-green negative granules, while in pathological sections of the AD group, diffuse orange-red positive staining granules were seen in the whole epidermal layer, especially in the spindled cell layer and the granular layer with the most significant staining intensity. Meanwhile, the positive staining granules of NFKB and STAT3 were expressed in the epidermis of the pathological sections of the AD group in a higher amount than that of the healthy group (Figure 1E).

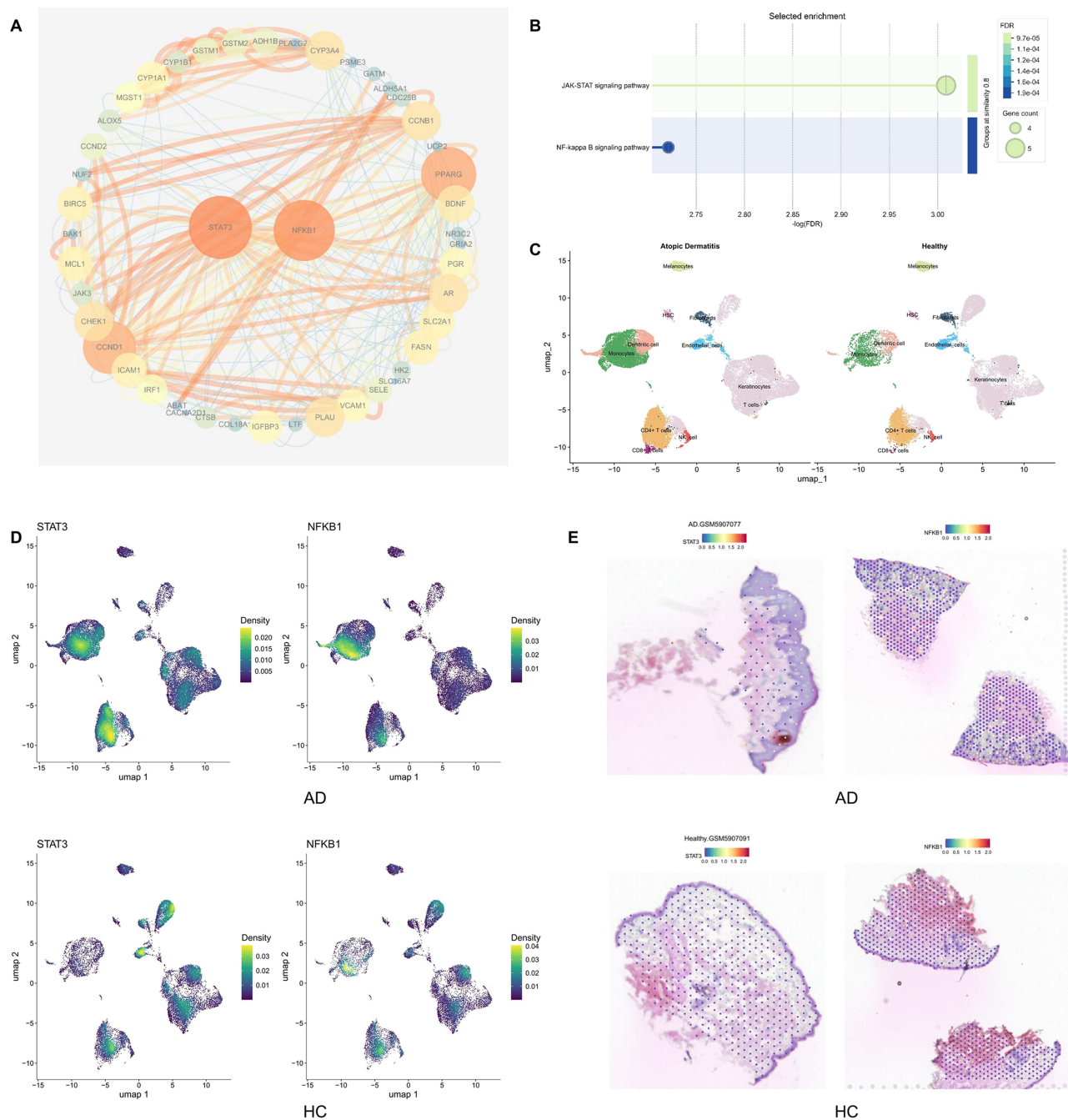


Figure 1 Using Bioinformatics to Predict Potential Targets for KSD in the Treatment of AD. **(A)** PPI network diagram (Node size and color intensity vary according to their Degree values). **(B)** KEGG enrichment of top 2 targets. **(C)** Analysis of cell subsets in GSE153760 single-cell sequencing. **(D)** NF-kB1 and STAT3 expression in t-SNE project. **(E)** NF-kB1 and STAT3 expression in Spatial transcriptomic datasets.

In conclusion, combined single-cell RNA sequencing and spatial transcriptome sequencing suggested that NF-kB and STAT3 may be important targets for KSD in the treatment of AD.

KSD Could Improve DNCB-Induced AD-Like Skin Lesions in Mice

During the intervention period (Figure 2A), the back skin of the normal mice was flesh pink in color, firm, smooth and elastic. As the time of external application of the modeling drug superimposed, the model mice successively developed typical symptoms of atopic dermatitis in the exposed skin, such as oozing, vesiculation, bleeding scabs, scratches and

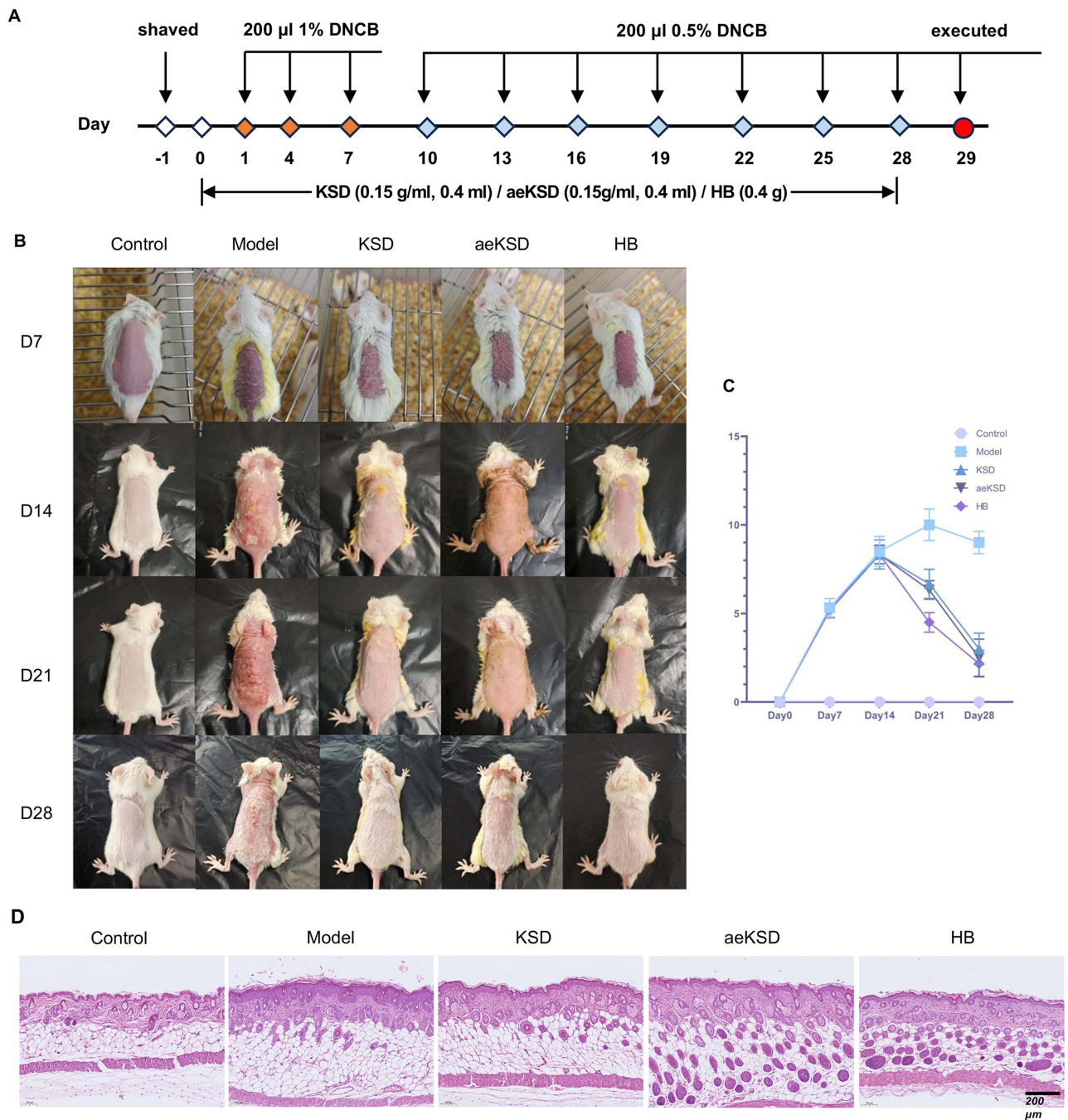


Figure 2 KSD could improve DNCB-induced AD-like skin lesions in mice. **(A)** The complete experimental procedure. **(B)** The typical pictures of mice in each group at different time points. **(C)** Dermatitis score in mice ($n = 6$). **(D)** Hematoxylin-Eosin staining of skin lesions in each group on day 28 ($n = 3$).

flaky desquamation. The remaining three groups of mice had varying degrees of neonatal hair, a few erythematous spots, and no obvious oozing, vesicles, haemorrhagic scabs, scratches or mossy lesions on the back skin. The typical skin lesions in each group of mice at different time spots are shown in Figure 2B.

As shown in Figure 2C, there were no abnormalities in the dorsal skin of the mice in all groups before the experiment, and the scores were all 0. At the 7th day of the experiment, except for the blank group, all groups of mice showed elevated skin lesion scores compared to control group ($p < 0.05$). However, there was no statistical difference between the model group and the experimental groups. At the 14th day of the experiment, all groups of mice showed a sustained

increase in skin lesion scores except for control group. There was still no statistical difference between the model group and experimental groups. At the 21st day of the experiment, the skin lesions in the model group continued to deteriorate. A downward trend in the skin lesion scores of mice was observed in all experimental groups after drug intervention and statistically different from that between the model groups. At the 28th day of the experiment, mice in the model group showed a slight downward trend in skin lesion scores. Symptoms of skin lesions in mice in all experimental groups continued to resolve and appeared statistically different from those in the model group.

Compared to control group, the epidermis of model group was significantly thickened compared with that of mice in the normal group. Pathological slides suggested there were hypertrophy of the epidermal stratum spinosum, hyperkeratosis, thickening of the stratum granulosum, perivascular inflammatory cell infiltration, and a small amount of eosinophilic granulocyte infiltration in model group. Inflammation was predominantly located in the stratum spinosum, hair follicles, and perivascular areas. Compared to model group, KSD, aeKSD and HB could reduce epidermal thickness of skin lesions in DNCB-induced AD mice and ameliorated inflammation (Figure 2D).

KSD Had Immunomodulatory Effects

Compared to the control group, increased number of mast cells with significant infiltration was seen in the model group ($p < 0.01$). KSD, aeKSD and HB could significantly reduce the number of mast cells compared to the model group ($p < 0.01$) (Figure 3A and B). It is known that mast cells can stimulate IgE secretion to some extent. The serum IgE level in each group was determined. Compared to control group, the serum IgE level was significantly elevated in model group ($p < 0.01$) but was decreased after intervention of KSD, aeKSD and HB ($p < 0.01$) (Figure 3C). Enlargement of the spleen generally signals hypersplenism and a surge in the immune response. As shown in Figure 3D, there was an increase in the spleen index in model group in comparison with control group ($p > 0.05$) and decrease in drug intervention groups compared with model group ($p > 0.05$).

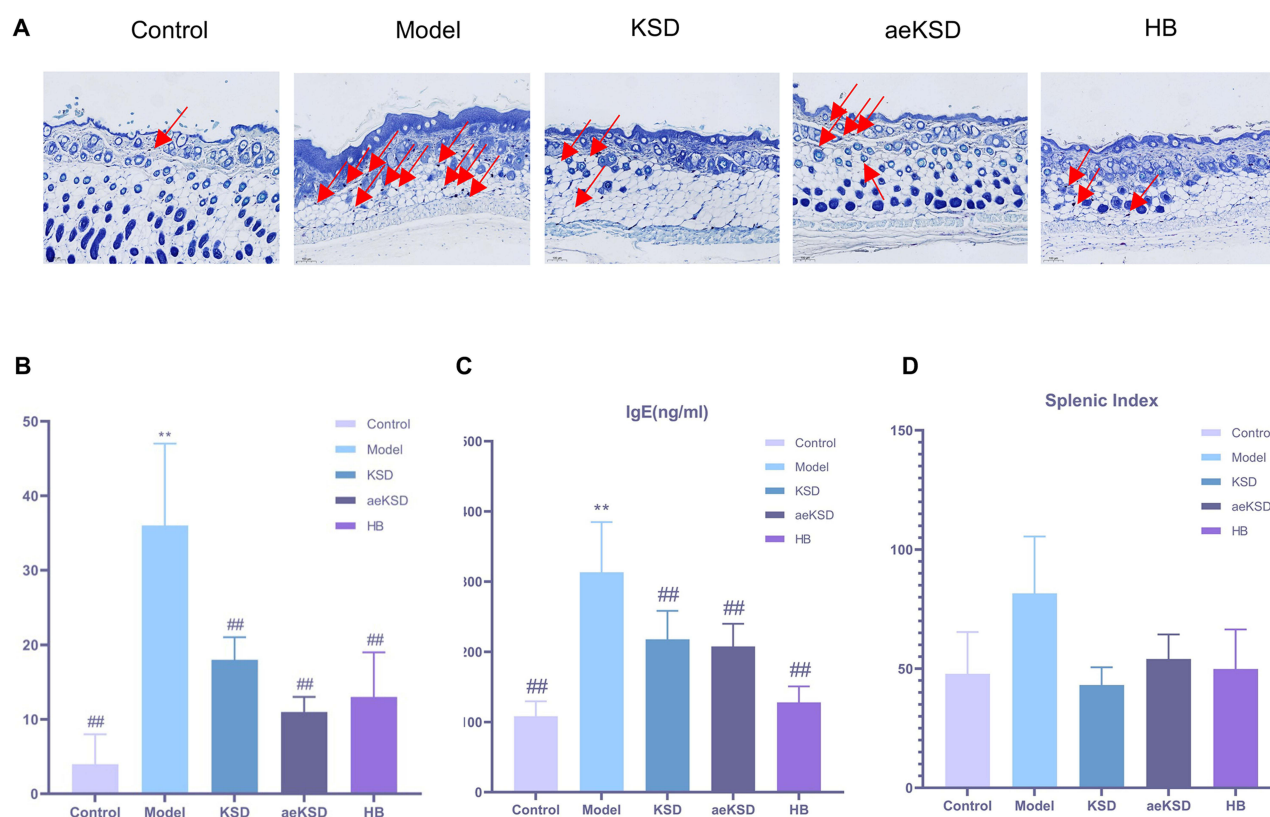


Figure 3 KSD had immunomodulatory effects on mast cells, which were marked with red arrows. **(A)** Toluidine-blue staining of mast cells ($n = 3$). **(B)** The number of mast cells in each group ($n = 3$). **(C)** The serum IgE level in each group ($n = 6$). **(D)** The splenic index in each group ($n = 6$). ** $P < 0.01$ vs Control group; ### $P < 0.01$ vs Model group.

KSD Could Improve Skin Barrier Function

Prior to sampling, skin elasticity, sebum content, pH, moisture content, skin temperature and melanin content were determined to evaluate the skin barrier function of DNCB-induced AD-like skin lesions. The skin barrier function of model group was severely impaired in comparison with control group, as evidenced by decrease in skin elasticity ($p < 0.01$), moisture content ($p < 0.01$) and melanin content ($p < 0.01$) and an increase in pH ($p < 0.05$) and skin temperature ($p < 0.01$). After drug intervention, the skin barrier function improved in skin elasticity, pH, moisture content, skin temperature and melanin content. However, there was no statistically significant difference between pharmacological intervention groups. Notably, no significant difference in sebum content between the groups was found (Figure 4A–F).

KSD Had No Liver or Kidney Toxicity

In order to investigate whether the intervention drug was hepatorenal toxic to mice, the livers and kidneys of mice in each group were collected and subjected to HE pathology staining to observe whether there were any abnormalities in the tissues. Comparison of the HE stained sections of the liver and kidney of each group, no abnormalities in the liver and kidney tissues was found.

HE staining of the liver of mice in all groups: the liver tissue structure was normal and complete. Hepatocytes were normal in morphology, with rounded nuclei, regular and dense arrangement, and were arranged in a cord-like pattern around the central vein, constituting the hepatic cord. No obvious pathology was observed. HE staining of kidneys of mice in all groups: renal tissue with normal morphology and integrity, clear nuclei, no inflammatory cell infiltration, intact glomerular structure, thin and clear vascular collaterals, and normal renal tubular structure (Figure 5A).

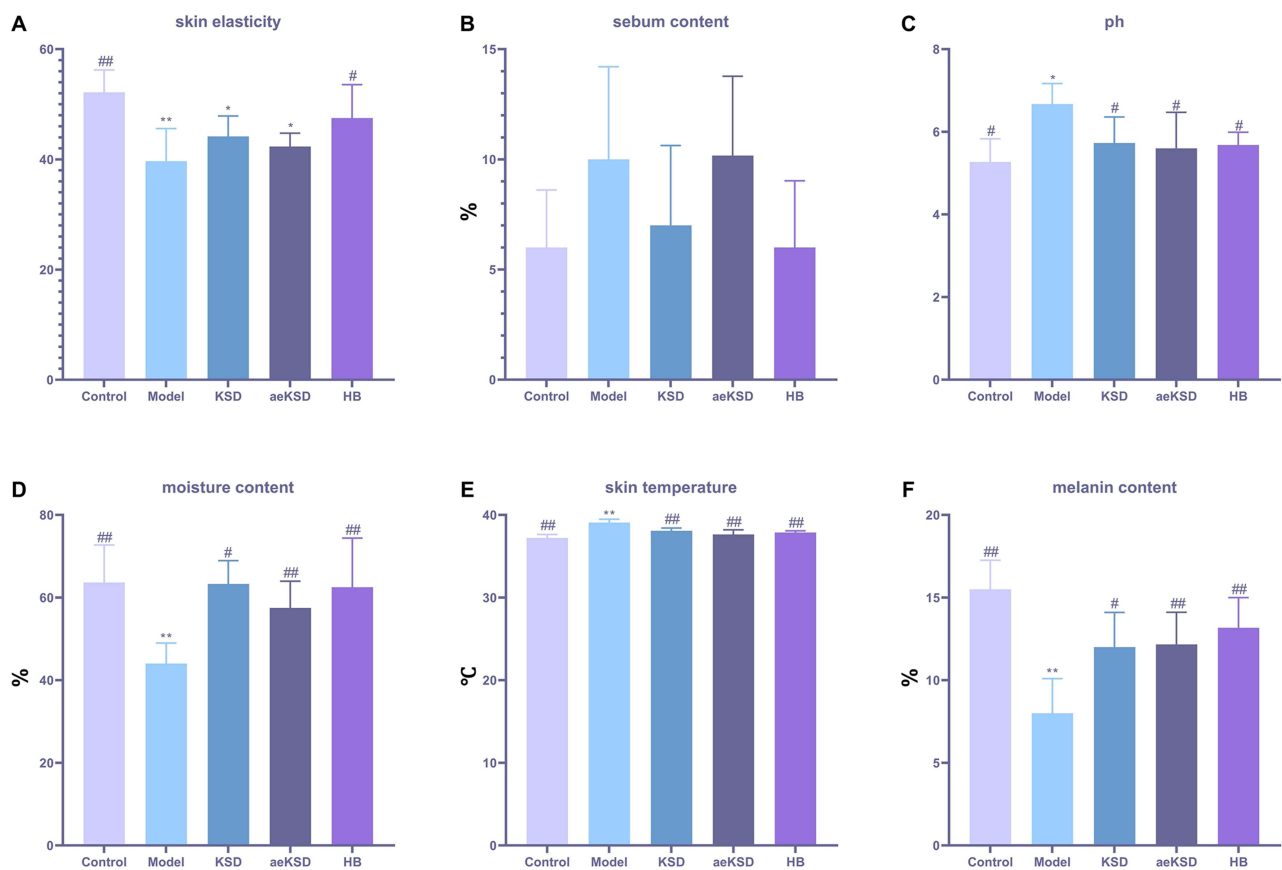


Figure 4 KSD could improve skin barrier function ($n = 6$). **(A)** The skin elasticity level in each group. **(B)** The sebum content level in each group. **(C)** The pH value in each group. **(D)** The moisture content in each group. **(E)** The skin temperature in each group. **(F)** The melanin content in each group. * $P < 0.05$, ** $P < 0.01$ vs Control group; # $P < 0.05$, ### $P < 0.01$ vs Model group.

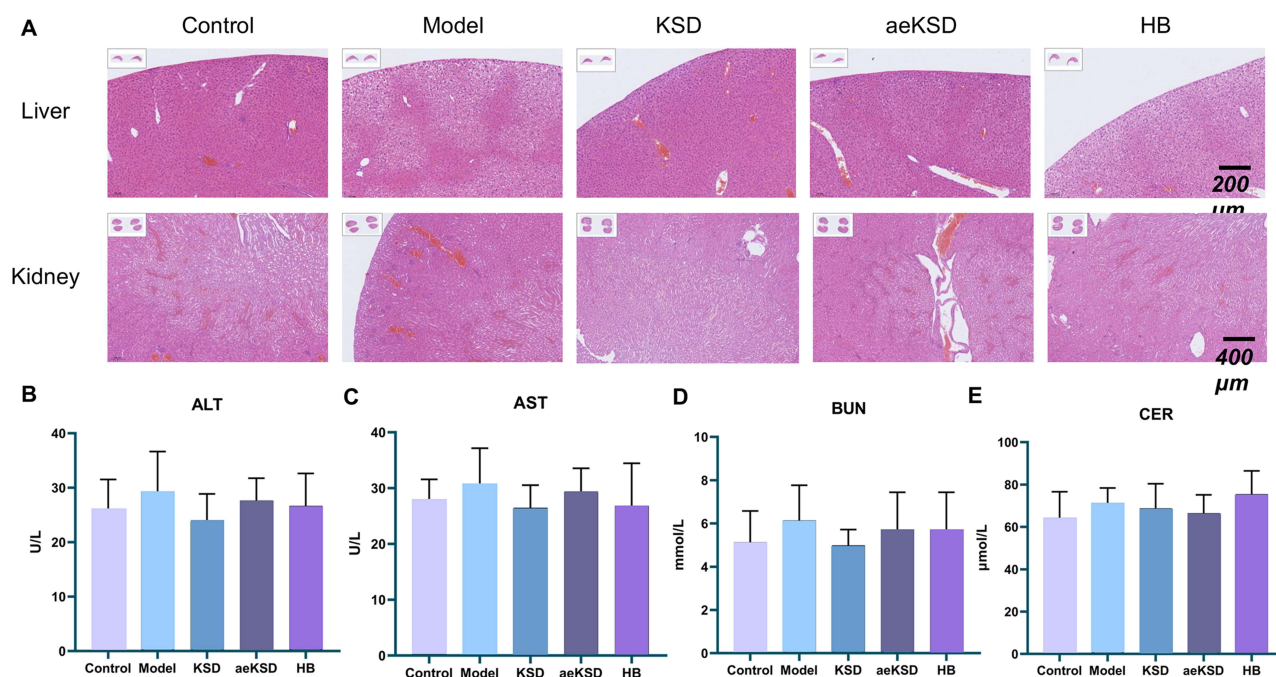


Figure 5 KSD had no liver or kidney toxicity. **(A)** Hematoxylin-Eosin staining of liver and kidney ($n = 1$). **(B)** The serum ALT level in each group ($n = 6$). **(C)** The serum AST level in each group ($n = 6$). **(D)** The serum BUN level in each group ($n = 6$). **(E)** The serum CER level in each group ($n = 6$).

The values of liver and kidney biochemical indexes did not show statistically significant differences between the groups, suggesting that the intervention drug has a good safety (Figure 5B–E).

NF- κ B Pathway and JAK-STAT3 Pathway May Be Potential Targets of KSD in the Treatment of AD

Flow cytometry assay was adopted to determine the amount of Th17 cells. An obvious increase in Th17 cell was demonstrated in the model group compared with control group ($p < 0.01$). The three intervention drugs decrease the Th17 cell level significantly in comparison with model group ($p < 0.01$) (Figure 6A and C).

Western Blot assay was used to detect the expression of key proteins in NF- κ B pathway and JAK-STAT3 pathway. Compared to control group, the expression of NF- κ B, p-NF- κ B p65, JAK2, p-JAK2, STAT3, p-STAT3 in the model group increased significantly ($p < 0.05$), while the three intervention groups all decrease the levels of aforementioned proteins ($p < 0.05$). Of the three medications, HB showed the best inhibition profile against aforementioned proteins ($p < 0.05$) (Figure 6B and D–F).

Discussion

AD is a complex, chronic inflammatory skin disease with a variety of therapeutic approaches with their own advantages and disadvantages. Current therapeutic strategies include topical and systemic therapies, which have limitations in terms of efficacy and safety.^{17,18} Recently, although biologics such as Dupilumab and JAK inhibitors such as Upadacitinib and Abrocitinib have emerged as emerging options for the treatment of AD,^{19,20} although dupilumab demonstrates a favorable safety profile, its mechanism primarily targets IL-4 and IL-13, which may result in suboptimal therapeutic efficacy for some patients, coupled with relatively high treatment costs. Meanwhile, the long-term safety validation of JAK inhibitors remains debatable, with expensive treatment expenses and potential adverse drug reactions including increased risk of infections.^{21,22} Therefore, topical treatment is usually the first choice for atopic dermatitis, and commonly used drugs include glucocorticoids and calcium-modulated phosphatase inhibitors. However, these drugs may trigger adverse effects, such as skin atrophy and burning sensation, leading to poor patient adherence.²³ Therefore, to explore new safe and long-term effective therapeutic strategies is of very significant value.

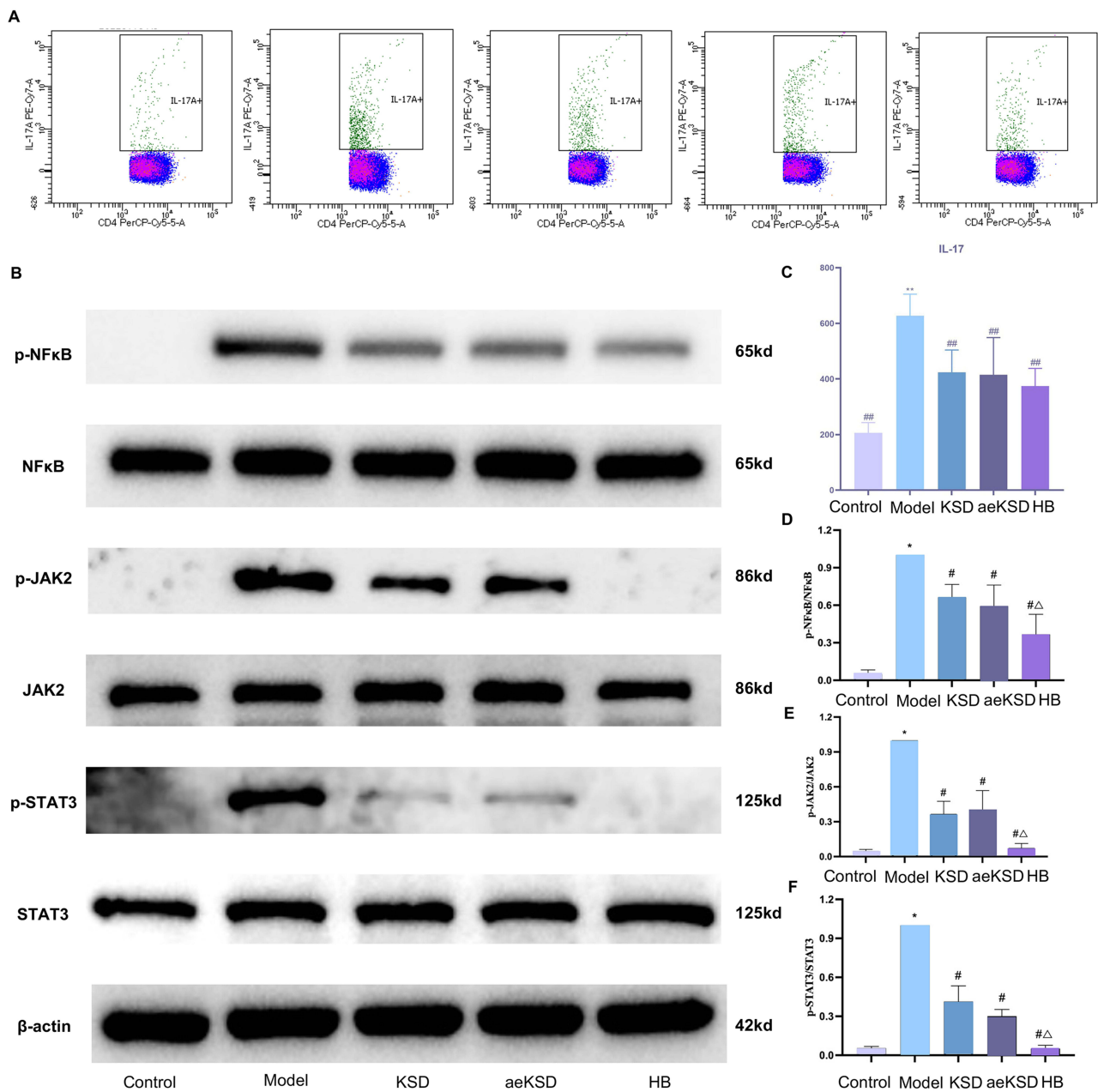


Figure 6 NF-κB pathway and JAK-STAT3 pathway may be the targets of KSD in the treatment of AD. **(A)** Flow cytometry assay was adopted to determine the amount of Th17 cells. **(B)** Western Blot assay was used to detect the expression of key proteins. **(C)** The Th17 cells in each group (n = 6). **(D)** The p-NFκB/NF-κB in each group (n = 3). **(E)** The p-JAK2/JAK2 in each group (n = 3). **(F)** The p-STAT3/STAT3 in each group (n = 3). *P < 0.05, **P < 0.01 vs Control group; #P < 0.05, ###P < 0.01 vs Model group; ΔP < 0.05 vs KSD group.

Given these limitations, TCM offers a promising complementary approach, owing to its characteristics of multiple components, multiple targets and multiple pathways. KSD, which was developed by famous veteran Chinese doctor-Jin Qifeng, has been used in Dongzhimen Hospital for several decades. This in-hospital preparation has been gaining good clinical efficacy. Exploiting its intrinsic therapeutic mechanism is of positive significance for the further development of pharmaceutical preparations. According to modern pharmacological studies, many ingredients in KSD are effective in suppressing inflammatory and regulating immune responses. For example, matrine, one of the main active ingredients in Ku Shen, has shown significant anti-inflammatory effects in a variety of inflammatory diseases. It was reported that matrine could regulate dendritic cell function²⁴ and inhibit JNK and NF-κB signaling pathways by upregulating miR-9.²⁵ Osthole, one of the main active ingredients in Shechuangzi, could inhibit the expression of inflammation-related proteins

through the regulation of multiple signaling pathways, thus exerting an anti-inflammatory effect.²⁶ In addition, flavonoids contained in Chuanjinpi also showed significant anti-inflammatory activity via regulating autophagy pathway.²⁷ These studies provide a theoretical foundation and experimental basis for the further development of KSD.

In our study, scRNA-seq and ST counts pinpoint potential targets for KSD in the treatment of AD, namely NF- κ B and STAT3 proteins. In subsequent animal experiments, we have confirmed that KSD had a therapeutic effect on DNCB-induced AD-like skin lesions by improving visible symptoms, such as erythema and scale. The number of mast cells, IgE level, skin barrier function, Th17 cells and NF- κ B and JAK-STAT3 signaling pathways all have improved. How KSD improves AD, by which pathways, either directly or indirectly, still remains unclear. However, the above mechanisms do play an important role in the development of the AD disease process.

The roles of NF- κ B and STAT3 in skin barrier function have been a hot research topic in recent years. The integrity of the skin barrier is essential for preventing the invasion of external pathogens and for maintaining the water balance of the skin. However, impairment of the skin barrier function is often associated with a variety of inflammatory skin diseases, such as atopic dermatitis and psoriasis. In these diseases, the NF- κ B and STAT3 signaling pathways are considered key regulators. STAT3 maintains skin barrier integrity by regulating SPINK5 and KLK5 expression in keratinocytes. Deficiency of STAT3 leads to the development of an inflammatory skin phenotype accompanied by increased itching and scratching behavior.²⁸ In addition, STAT3 is involved in the formation of TSLP-induced epidermal barrier defects by forming a complex with IL-33.²⁹ In rosacea research, STAT3 has been identified as a central regulatory gene for skin barrier dysfunction, which exacerbates the inflammatory response by activating cytokine signaling pathways.³⁰ On the other hand, the role of the NF- κ B signaling pathway in skin inflammation cannot be ignored. In studies of AD, miR-1294 reduced oxidative stress-dependent inflammatory responses by inhibiting the STAT3/NF- κ B pathway, thereby improving skin barrier function.³¹ In summary, NF- κ B and STAT3 have important roles in the regulation of skin barrier function. They are not only involved in the maintenance of the skin barrier but also play a key role in the pathological process of skin inflammatory diseases.

The NF- κ B and STAT3 signaling pathways play key roles in the differentiation and function of Th17 cells, an important subpopulation of helper T cells that participate in the immune response and inflammatory response by secreting cytokines such as IL-17. In recent years, therapeutic strategies targeting Th17 cells have evolved in the treatment of AD aiming to offer more personalized treatment options for patients.³² Dexamethasone is able to effectively reduce the proportion of Th17/1 cells by inhibiting the phosphorylation of NF- κ B and STAT3, and thus may be a potential therapeutic strategy for correcting the Th17/1 cell bias in idiopathic thrombocytopenic purpura.³³ In inflammatory skin diseases such as psoriasis, IL-17A and IL-36 γ promote interactions between keratinocytes and endothelial cells through activation of the NF- κ B and STAT3 signaling pathways, thereby maintaining inflammation.³⁴ In addition, α 7 nicotinic acetylcholine receptor agonists are able to attenuate psoriasis-like inflammation by inhibiting STAT3 and NF- κ B signaling pathways.³⁵ Therefore, modulating the activity of NF- κ B and STAT3 signaling pathways has emerged as a potential therapeutic strategy for a variety of diseases.

Furthermore, the interaction between NF- κ B and STAT3 may have an important regulatory role in mast cells. In mast cells, IL-33 promotes ICAM-1 expression through the NF- κ B pathway, which in turn enhances cell adhesion, suggesting the importance of NF- κ B in mast cell inflammatory responses.³⁶ Berberine significantly reduced IL-33-induced mast cell inflammatory responses by inhibiting the NF- κ B and p38 signaling pathways, further supporting the critical role of NF- κ B in mast cell functions.³⁷ Mitochondrial STAT3 was found to play a major role in IgE antigen-mediated mast cell cytokinesis, which regulates cellular function by promoting oxidative phosphorylation activity.³⁸ Furthermore, mutations in STAT3 were associated with a reduction in anaphylaxis, suggesting the importance of STAT3 signaling in mast cell degranulation.³⁹

Taken together, NF- κ B and STAT3 signaling pathways has very closed relationship with AD. In our study, it was obvious that KSD did have effects on NF- κ B and STAT3, while it cannot yet be assumed that KSD has a direct regulatory effect on NF- κ B and STAT3. Follow-up knockout experiments are necessary.

KSD is a preparation containing ethanol. In order to explore the influence of ethanol, aeKSD (without ethanol) was prepared too. It was found that KSD was better improving scale, and aeKSD was better improving erythema. KSD performed better in improving skin barrier function, number of mast cell, IgE level and target proteins. The reason may be that tinctures are inhibitory to bacterial flora and could promote drug absorption. Every coin has two sides. Tinctures can

be irritating to wounds formed by prolonged scratching, and long-term use of tinctures can have side effects on normal skin. In addition, tinctures evaporate more quickly and the drug has a shorter residence time, which also diminishes the efficacy of the drug. In order to solve these problems, follow up with dosage form improvements is needed.

In addition to innovations in the drugs themselves, advances in drug delivery systems offer new hope for the treatment of atopic dermatitis. Nanotechnology and other advanced drug delivery systems can increase the stability and bioavailability of drugs, reduce side effects and improve patient compliance.⁴⁰ For example, delivery systems such as liposomes, gels and microneedles allow for deep skin penetration and controlled release of drugs, leading to improved therapeutic outcomes.^{41,42}

Conclusions

In summary, our study investigates the role and mechanisms of KSD in alleviating DNCB-induced AD by combining scRNA-seq, ST and experimental validation. Our findings reveal that KSD has therapeutic effects on DNCB-induced AD-like skin lesions and its possible targets maybe NF- κ B and JAK-STAT3 proteins.

Highlights

- KSD significantly improved DNCB-induced AD-like dermatitis in mice with good safety.
- NF- κ B and JAK-STAT3 signaling pathways may be potential targets of KSD.

Abbreviations

KSD, Kushe tincture; DNCB, 2,4-Dinitrochlorobenzene; AD, Atopic dermatitis; aeKSD, KSD alcoholic extract; ScRNA-seq, Single-cell RNA sequencing; ST, Spatial transcriptomics; TCMSP, Traditional Chinese Medicine Systems Pharmacology; GEO, Gene Expression Omnibus; PPI, Protein-protein interaction; KEGG, Kyoto encyclopedia of genes and genomes; TCM, Traditional Chinese medicine; PCA, Principal component analysis; UMAP, Uniform manifold approximation and projection; SNN, Shared Nearest Neighbour; PMSF, Phenylmethanesulfonyl fluoride; SCORAD, Scoring atopic dermatitis; H&E, Hematoxylin-eosin staining; OD, Optical density; WB, Western blot; ALT, Alanine aminotransferase; AST, Aspartate transaminase; BUN, Blood urea nitrogen; CER, Creatinine.

Data Sharing Statement

The data that support the findings of this study are available from the corresponding author upon reasonable request.

Ethical Approval

All experiments were conducted in accordance with the ARRIVE guidelines and carried out in strict accordance with the National Institutes of Health Guide for the Care and Use of Laboratory Animals. The animals were treated in accordance with the Guidelines for Ethical Review of Experimental Animal Welfare (GB/T35892-2018) issued by China. Due to the long scheduling cycle of animal experiments at our affiliated hospital's animal facility, and as most experiments were conducted outside regular working hours, we utilized the animal laboratory of the contracted company (where we procure experimental animals and reagents) to carry out our studies. Consequently, the animal ethics review was conducted by the ethics committee of Beijing MDKN Biotechnology Co., Ltd (Approval No. MDKN-2022-079). In addition, the GeneCards and GEO are public databases whose data contributors have provided prior ethical consent for research use. Researchers may freely utilize these resources for data acquisition and subsequent publication. In this study, we legally utilized the public database (GEO) for our research. In accordance with Item 1 and Item 2 of Article 32 of the "Measures for Ethical Review of Life Science and Medical Research Involving Human Subjects" issued in China on February 18, 2023, this study is eligible for ethical exemption.

Author Contributions

Huishang Feng: Funding acquisition, Methodology, Project administration, Writing-original draft and Writing-review and editing; Yang Zhou: Formal analysis, Software, Validation and Visualization, Data analysis. Xuewen Ren: Conceptualization,

Investigation and Writing-original draft; Xintian Zhu: Data curation, Formal analysis and Resources; Baochen Zhu: Data curation, Formal analysis and Resources;

Xingwu Duan: Resources, Supervision and Validation; Shuangqing Qu: Resources, Supervision and Validation; Yuanwen Li: Data curation, Formal analysis, Methodology, Resources, Supervision and Writing-review and editing. Yeping Qin: Data curation, Formal analysis, Methodology, Resources, Supervision and Writing-review and editing. All authors took part in drafting, revising or critically reviewing the article; gave final approval of the version to be published; have agreed on the journal to which the article has been submitted; and agree to be accountable for all aspects of the work. To ensure the proper implementation of the blinding procedure in the experiment, Huishang Feng is responsible for subject allocation, Xuewen Ren for experimental implementation, Yeping Qin for outcome assessment, and Yang Zhou for data analysis.

Funding

This study was supported by Beijing University of Chinese Medicine Scientific Research Project (No. 2024-JYB-JBZD-018 & 2020-JYB-XJSJJ-044).

Disclosure

The authors confirmed that there are no conflicts of interest related to this publication.

References

1. Yang EJ, Sekhon S, Sanchez IM, Beck KM, Bhutani T. Recent developments in atopic dermatitis. *Pediatrics*. 2018;142(4). doi:10.1542/peds.2018-1102
2. Nutten S. Atopic dermatitis: global epidemiology and risk factors. *Ann Nutr Metab*. 2015;66(1):8–16. doi:10.1159/000370220
3. Guo Y, Zhang H, Liu Q, et al. Phenotypic analysis of atopic dermatitis in children aged 1-12 months: elaboration of novel diagnostic criteria for infants in China and estimation of prevalence. *J Eur Acad Dermatol*. 2019;33(8):1569–1576. doi:10.1111/jdv.15618
4. Zhang R, Zhang H, Shao S, et al. Compound traditional Chinese medicine dermatitis ointment ameliorates inflammatory responses and dysregulation of itch-related molecules in atopic dermatitis. *Chin Med*. 2022;17(1):3. doi:10.1186/s13020-021-00555-7
5. Duan XW, Qu SQ. Records of jin qifeng's clinical cases and experience. *China Medical Science*. 2022;2022.
6. Ma GR. Experience of Jin qifeng in treating blood heat psoriasis. *China's Naturopathy*. 2016;24(06):13.
7. Huang Y, Li X, Zhang X, Tang J. 2020 Oxymatrine ameliorates memory impairment in diabetic rats by regulating oxidative stress and apoptosis: involvement of NOX2/NOX4. *Oxid Med Cell Longev*. 2020;3912173. doi:10.1155/2020/3912173
8. Lan X, Zhao J, Zhang Y, Chen Y, Liu Y, Xu F. Oxymatrine exerts organ- and tissue-protective effects by regulating inflammation, oxidative stress, apoptosis, and fibrosis: from bench to bedside. *Pharmacol Res*. 2019;151104541. doi:10.1016/j.phrs.2019.104541
9. Xiang X, Tu C, Li Q, et al. Oxymatrine ameliorates imiquimod-induced psoriasis pruritus and inflammation through inhibiting heat shock protein 90 and heat shock protein 60 expression in keratinocytes. *Toxicol Appl Pharm*. 2020;405115209. doi:10.1016/j.taap.2020.115209
10. Matsuda H, Tomohiro N, Ido Y, Kubo M. Anti-allergic effects of cnidii monnieri fructus (dried fruits of *Cnidium monnieri*) and its major component, osthol. *Biol Pharm Bull*. 2002;25(6):809–812. doi:10.1248/bpb.25.809
11. Zhai XT, Chen JQ, Jiang CH, et al. *Corydalis bungeana* Turcz. attenuates LPS-induced inflammatory responses via the suppression of NF- κ B signaling pathway in vitro and in vivo. *J Ethnopharmacol*. 2016;194:153–161. doi:10.1016/j.jep.2016.09.013
12. Mitamura Y, Reiger M, Kim J, et al. Spatial transcriptomics combined with single-cell RNA-sequencing unravels the complex inflammatory cell network in atopic dermatitis. *Allergy*. 2023;78(8):2215–2231. doi:10.1111/all.15781
13. Xia T, Liang X, Liu CS, Hu YN, Luo ZY, Tan XM. Network pharmacology integrated with transcriptomics analysis reveals ermiao wan alleviates atopic dermatitis via suppressing MAPK and activating the EGFR/AKT signaling. *Drug Des Devel Ther*. 2022;16:4325–4341. doi:10.2147/DDDT.S384927
14. Zhang X, Ding C, Zhao Z. Identification of diagnostic molecules and potential therapeutic agents for atopic dermatitis by single-cell RNA sequencing combined with a systematic computing framework that integrates network pharmacology. *Funct Integr Genomics*. 2023;23(2):95. doi:10.1007/s10142-023-01005-3
15. Yu K, Wang Y, Wan T, et al. Tacrolimus nanoparticles based on chitosan combined with nicotinamide: enhancing percutaneous delivery and treatment efficacy for atopic dermatitis and reducing dose. *Int J Nanomed*. 2017;13:129–142. doi:10.2147/IJN.S150319
16. Qin C, Wang F, Zhang Z, et al. The effects of lianzhuyin on Th17/treg immune imbalance and aromatic hydrocarbon receptor expression in atopic dermatitis mice. *Chin J Dermatovenereol*. 2024;38(08):837–848. doi:10.13735/j.cjdv.1001-7089.202311119
17. Silverberg JI. Atopic dermatitis treatment: current state of the art and emerging therapies. *Allergy Asthma Proc*. 2017;38(4):243–249. doi:10.2500/aap.2017.38.4054
18. Zhang Y, Yuan S, Wu Y, et al. Advancements in pharmacological interventions for atopic dermatitis current strategies and future directions. *Inflammopharmacology*. 2025;33(3):1221–1236. doi:10.1007/s10787-025-01659-4
19. Ferreira S, Guttman-Yassky E, Torres T. Selective JAK1 inhibitors for the treatment of atopic dermatitis: focus on upadacitinib and abrocitinib. *Am J Clin Dermatol*. 2020;21(6):783–798. doi:10.1007/s40257-020-00548-6
20. McGregor S, Farhangian ME, Feldman SR. Dupilumab for the treatment of atopic dermatitis: a clinical trial review. *Expert Opin Biol Ther*. 2015;15(11):1657–1660. doi:10.1517/14712598.2015.1076388
21. Chiricoczi A, Gori N, Maurelli M, et al. Biological agents targeting interleukin-13 for atopic dermatitis. *Expert Opin Biol Ther*. 2022;22(5):651–659. doi:10.1080/14712598.2022.2035356

22. Hasan I, Parsons L, Duran S, et al. Dupilumab therapy for atopic dermatitis is associated with increased risk of cutaneous T cell lymphoma: a retrospective cohort study. *J Am Acad Dermatol.* 2024;91(2):255–258. doi:10.1016/j.jaad.2024.03.039
23. Ghosalkar S, Singh P, Ravikumar P. Emerging topical drug delivery approaches for the treatment of Atopic dermatitis. *J Cosmet Dermatol-U.S.* 2021;21(2):536–549. doi:10.1111/jocd.14685
24. Li N, Zhao J, Di T, et al. Matrine alleviates imiquimod-induced psoriasisform dermatitis in BALB/c mice via dendritic cell regulation. *Int J Clin Exp Pathol.* 2018;11(11):5232–5240. PMID: 31949603.
25. Jiang J, Wang G. Matrine protects PC12 cells from lipopolysaccharide-evoked inflammatory injury via upregulation of miR-9. *Pharm Biol.* 2020;58(1):314–320. doi:10.1080/13880209.2020.1719165
26. Zafar S, Sarfraz I, Rasul A, et al. Osthole: a multifunctional natural compound with potential anticancer, antioxidant and anti-inflammatory activities. *Mini-Rev Med Chem.* 2021;21(18):2747–2763. doi:10.2174/1389557520666200709175948
27. Kan LL, Liu D, Chan BC, et al. The flavonoids of sophora flavescens exerts anti-inflammatory activity via promoting autophagy of bacillus calmette-guérin-stimulated macrophages. *J Leukocyte Biol.* 2020;108(5):1615–1629. doi:10.1002/JLB.3MA0720-682RR
28. Kim J, Kim MG, Jeong SH, et al. STAT3 maintains skin barrier integrity by modulating SPINK5 and KLK5 expression in keratinocytes. *EXP DERMATOL.* 2021;31(2):223–232. doi:10.1111/exd.14445
29. Dai X, Muto J, Shiraishi K, et al. TSLP impairs epidermal barrier integrity by stimulating the formation of nuclear IL-33/phosphorylated STAT3 complex in human keratinocytes. *J Invest Dermatol.* 2022;142(8):2100–2108.e5. doi:10.1016/j.jid.2022.01.005
30. Wang Y, Wang B, Huang Y, et al. Multi-transcriptomic analysis and experimental validation implicate a central role of STAT3 in skin barrier dysfunction induced aggravation of rosacea. *J Inflamm Res.* 2022;15:2141–2156. doi:10.2147/JIR.S356551
31. Yan C, Ying J, Lu W, et al. MiR-1294 suppresses ROS-dependent inflammatory response in atopic dermatitis via restraining STAT3/NF-κB pathway. *CELL IMMUNOL.* 2021;371(104452). doi:10.1016/j.cellimm.2021.104452
32. Na CH, Baghoomian W, Simpson EL. A therapeutic renaissance - emerging treatments for atopic dermatitis. *Acta Derm-Venereol.* 2020;100(12):adv00165. doi:10.2340/00015555-3515
33. Li J, Hua M, Hu X, et al. Dexamethasone suppresses the Th17/1 cell polarization in the CD4+ T cells from patients with primary immune thrombocytopenia. *THROMB RES.* 2020;190:26–34. doi:10.1016/j.thromres.2020.04.004
34. Mercurio L, Failla CM, Capriotti L, et al. Interleukin (IL)-17/IL-36 axis participates to the crosstalk between endothelial cells and keratinocytes during inflammatory skin responses. *PLoS One.* 2020;15(4):e0222969. doi:10.1371/journal.pone.0222969
35. Chen Y, Lian P, Peng Z, et al. Alpha-7 nicotinic acetylcholine receptor agonist alleviates psoriasis-like inflammation through inhibition of the STAT3 and NF-κB signaling pathway. *Cell Death Discov.* 2022;8(1):141. doi:10.1038/s41420-022-00943-4
36. Numata T, Ito T, Maeda T, et al. IL-33 promotes ICAM-1 expression via NF-κB in murine mast cells. *Allergol Int.* 2015;65(2):158–165. doi:10.1016/j.alit.2015.10.004
37. Li W, Yin N, Tao W, et al. Berberine suppresses IL-33-induced inflammatory responses in mast cells by inactivating NF-κB and p38 signaling. *Int Immunopharmacol.* 2018;66:82–90. doi:10.1016/j.intimp.2018.11.009
38. Erlich TH, Yagil Z, Kay G, et al. Mitochondrial STAT3 plays a major role in IgE-antigen-mediated mast cell exocytosis. *J Allergy Clin Immunol.* 2014;134(2):460–469. doi:10.1016/j.jaci.2013.12.1075
39. Siegel AM, Stone KD, Cruse G, et al. Diminished allergic disease in patients with STAT3 mutations reveals a role for STAT3 signaling in mast cell degranulation. *J Allergy Clin Immunol.* 2013;132(6):1388–1396. doi:10.1016/j.jaci.2013.08.045
40. Parekh K, Mehta TA, Dhas N, et al. Emerging nanomedicines for the treatment of atopic dermatitis. *AAPS Pharm Sci Tech.* 2021;22(2):55. doi:10.1208/s12249-021-01920-3
41. Krysiak ZJ, Stachewicz U. Electrospun fibers as carriers for topical drug delivery and release in skin bandages and patches for atopic dermatitis treatment. *Wires Nanomed Nanobi.* 2022;15(1):e1829. doi:10.1002/wnan.1829
42. Ali S, Ion A, Orzan OA, et al. Emerging treatments and new vehicle formulations for atopic dermatitis. *Pharmaceutics.* 2024;16(11).

Journal of Inflammation Research

Publish your work in this journal

The Journal of Inflammation Research is an international, peer-reviewed open-access journal that welcomes laboratory and clinical findings on the molecular basis, cell biology and pharmacology of inflammation including original research, reviews, symposium reports, hypothesis formation and commentaries on: acute/chronic inflammation; mediators of inflammation; cellular processes; molecular mechanisms; pharmacology and novel anti-inflammatory drugs; clinical conditions involving inflammation. The manuscript management system is completely online and includes a very quick and fair peer-review system. Visit <http://www.dovepress.com/testimonials.php> to read real quotes from published authors.

Submit your manuscript here: <https://www.dovepress.com/journal-of-inflammation-research-journal>

Dovepress
Taylor & Francis Group